FINAL TECHNICAL REPORT

Rapid finite-fault earthquake and afterslip information from seismic and real-time GPS observations

Award Number:	**G12AP20097**
Start Date & End Date:	6/2012 – 5/2013

Principal Investigator:	Douglas S Dreger
Email Address:	dreger@seismo.berkeley.edu
Co-Principal Investigator:	Ingrid Johanson
Email Address:	ingrid@seismo.berkeley.edu
Institution and Address:	University of California, Berkeley Berkeley Seismological Laboratory 215 McCone Hall # 4760 Berkeley, CA 94720-4760

Abstract

We have developed a strategy to use real-time GPS data access with rapid post-processing techniques to estimate static offsets from moderate to large earthquakes and use them to constrain a non-linear search for fault plane parameters. Rapid post-processing requires waiting 1-2 minutes after the earthquake for data to accumulate, but displacement time series can then be generated within 5 minutes using the software Track, developed at MIT. From these, full fault plane determination can be performed within another 5 minutes. While real-time processing techniques are critical for using GPS data for Earthquake Early Warning, rapid post-processing provides higher precision in the static offset measurement. This allows GPS data to be used for smaller earthquakes and still finishes within a time frame appropriate for ShakeMap. Finite fault effects have been shown to be an important part of ShakeMap; they allow improved estimates of shaking near the fault and due to rupture directivity.

Rapid finite-fault earthquake and afterslip information from seismic and real-time GPS observations

Award Number: **G12AP20097**

Douglas Dreger
Ingrid Johanson
University of California, Berkeley
Department of Earth and Planetary Science
307 McCone Hall
Berkeley, CA 94720-4767
Telephone: (510) 545-3525;
Fax:(510) 643-5811;
E-mail: ingrid@seismo.berkeley.edu

Introduction

Rapid access to reliable earthquake information is critical for emergency response. In the case of a major earthquake, the mobilization of local, state, and federal disaster operations can be greatly enhanced by dependable, near real-time estimates of location, magnitude, mechanism, and extent of strong ground shaking. Over the last decade, ShakeMap - a representation of the distribution of earthquake peak ground motion and intensity - has emerged as a critical product for emergency response operations, and is valued by emergency response personnel [*Wald et al.*, 1999; 2008]. It provides information that can be used to identify endangered communities, to evaluate the impact on lifelines, and to provide input for damage and loss estimation. Current applications of rapid earthquake information include the emergency services, transportation, utilities, telecommunications, and insurance industries.

ShakeMaps, originally developed as part of the TriNet Project in southern California [*Wald et al.*, 1999], combine observed ground motions (PGA, PGV, and spectral acceleration) with attenuation relations to produce maps showing the distribution of shaking. The attenuation-based shaking model is used to fill in where there is less data and to interpolate between data points and is by default calculated from the distance to the earthquake hypocenter. However, for large earthquakes a simple parameterization of shaking based on hypocentral distance does not provide complete information for post-earthquake response. The finite extent of the source and the effects of directivity become important for larger events. Accounting for finite fault effects,

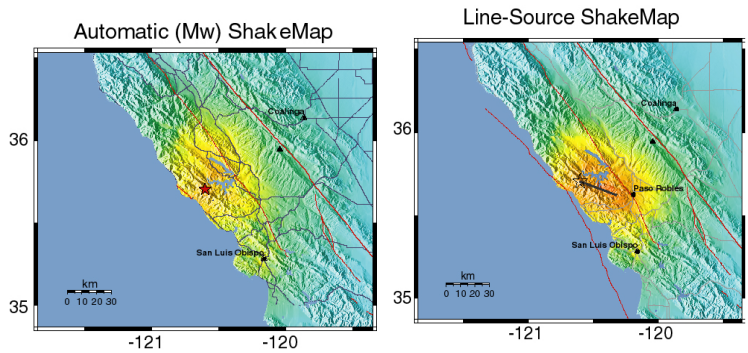

Figure 1. Comparison of ShakeMaps for the 2003 M_W6.5 San Simeon earthquake. Shown are rapid determinations based on only a few seismic stations. Left, standard point-source attenuation models; right, models that include adjustments based on the automated line-source model. The finite source model extends and increases the predicted intensities to the southeast, in agreement with observations.

through line source and finite fault modeling (Figure 1), has provided a marked improvement in ShakeMap in many cases [*Dreger et al.*, 2005]. ShakeMap can also use the finite fault information directly. Given rupture dimensions, ShakeMap can instead calculate station distance to the fault plane, which allows higher levels of shaking throughout the rupture area. Including a finite fault plane in ShakeMap already happens for large earthquakes, however it is not yet automated and requires manual intervention to determine the rupture plane and add it to the processing. With real-time GPS data and rapid post-processing, finite fault parameters are automatically determined and can be provided to ShakeMap within 20 minutes.

Seismic monitoring in California and rapid earthquake information

In Northern California, the University of California, Berkeley Seismological Laboratory (BSL) and the USGS Menlo Park collaborate closely to provide timely and reliable earthquake information to the federal, state, and local governments, to public and private agencies, to researchers nation- and worldwide and to the general public. This collaboration forms the Northern California Earthquake Management Center (NCEMC) of the CISN. The CISN is a partnership among the USGS, California Geological Survey, UC Berkeley, and Caltech, combining efforts in northern and southern California as well as weak and strong motion networks. The NCEMC uses the ANSS Quake Management System (AQMS, formerly called the CISN software) to routinely produce estimates of earthquake location and magnitude within 2-4 minutes after an event. For events of magnitude 3.5 and larger, the CISN centers also produce ShakeMaps within 6-8 minutes.

In 2010 the BSL signed a MOU with the USGS, Menlo Park to share GPS data and to cooperate in providing information to earthquake response products from GPS. An important aspect of NCEDC is that the BSL and USGS processing centers mirror each other, providing mutual back-ups in the case that either center goes offline. In order to incorporate GPS information into CISN, similar mirrored processing will need to be in place for GPS data.

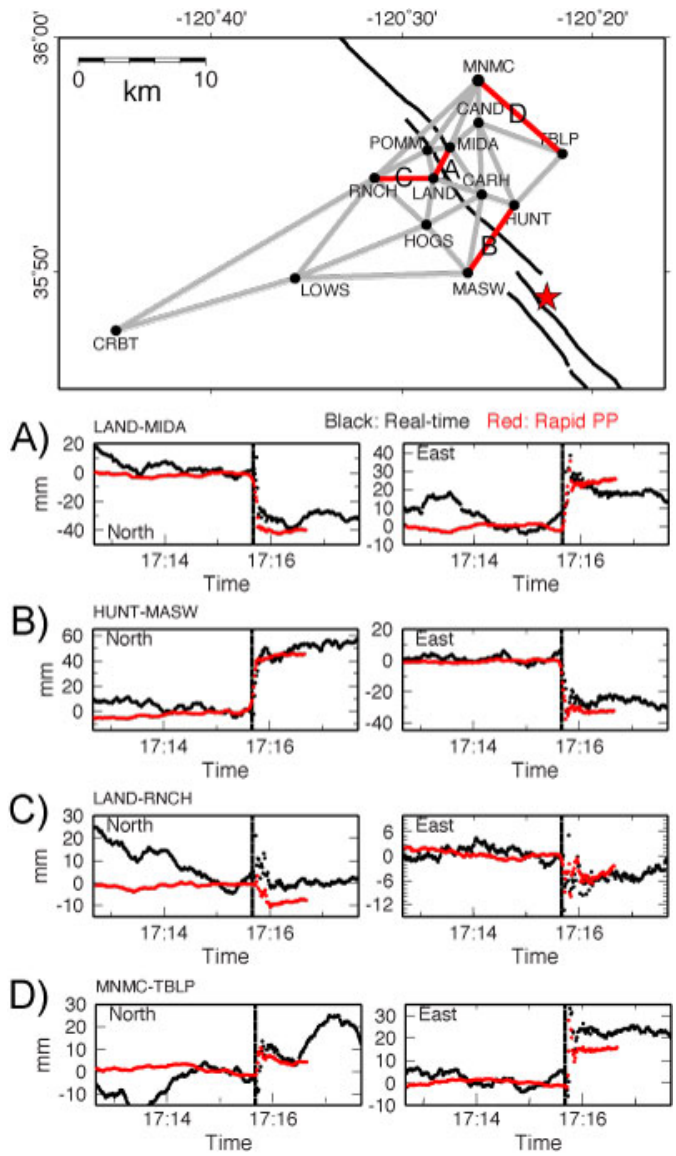

Figure 2: A comparison of simulated real-time (black) and rapid post-processing (red) GPS time series for four baselines during the 2004 Parkfield earthquake. Top panel shows the triangulated processing network in grey, with the four baselines shown highlighted in red. The vertical line shows the origin time of the earthquake.

Geodetic Observations

Although seismic networks can be used to estimate finite-fault parameters, they often have poor sensitivity to the geometry of the rupture. Geodetic networks, particularly if they have stations close to the event, often have much better sensitivity to the orientation and areal extent of rupture, providing a complementary data source for independently estimating rupture parameters of M>6 events. High-rate (1 Hz sampling) GPS data also provide information at low frequencies and for static offsets, information that is difficult to obtain from seismometers [*Larson et al.*, 2003].

Geodetic measurements of coseismic displacements provide important constraints on earthquake faulting, including the location and extent of the rupture plane, unambiguous resolution of the nodal plane, and the distribution of slip on the fault unbiased by rupture velocity assumptions [e.g. *Murray-Moraleda and Simpson*, 2009; *Johanson and Bürgmann*, 2010]. Seismic and geodetic observations can also be inverted simultaneously to improve resolution of finite-fault earthquake source models [*Rolandone et al.*, 2006; *Kim and Dreger*, 2008]. These and other studies typically find that the geodetic data is most sensitive to the fault geometry and provides a smooth slip distribution, and that the seismic data resolves the temporal evolution of the slip including rupture and slip velocity variations, and smaller scale heterogeneity in the slip distribution [e.g. *Cohee and Beroza*, 1994]. For example, *Chi et al.* (2001) found that GPS data were critical for constraining the complex geometry of the northern end of the rupture zone in the Chi-Chi earthquake where the rupture bends to the east.

Rapid Post-processing

Under this award, we have developed a methodology to use GPS data to provide static offsets and finite fault parameters that can be used for ShakeMap. While we originally planned to use real-time processing techniques, we soon realized that more precise results could be obtained with high-rate post-processing. Even by waiting as little as 1 minute, better estimates of static offset and smaller offsets can be obtained than with real-time processing. Rapid post-processing (RPP) requires waiting 1-2 minutes after the earthquake for data to accumulate, but displacement time series can then be generated within 5 minutes using Track, a freely-available, open-source processing package developed at MIT. From these, full fault plane determination can be performed within another 5 minutes. While real-time processing techniques are critical for using GPS data for Earthquake Early Warning, the more accurate RPP allows GPS data to be used for smaller earthquakes and still finishes within a time frame appropriate for ShakeMap.

We use the 2004 M6.0 Parkfield earthquake as a test case and find that RPP with Track allows more robust static offset determination from this moderate sized earthquake than real-time processing (Figure 2). We compare both simulated real-time processing using TrackRT rewind (black) and simulated RPP with Track (red), using abbreviated data files and predicted orbit products. While both real-time and RPP capture the largest offsets, smaller offsets are better captured by RPP. This is especially evident for non-fault crossing pairs such as C and D.

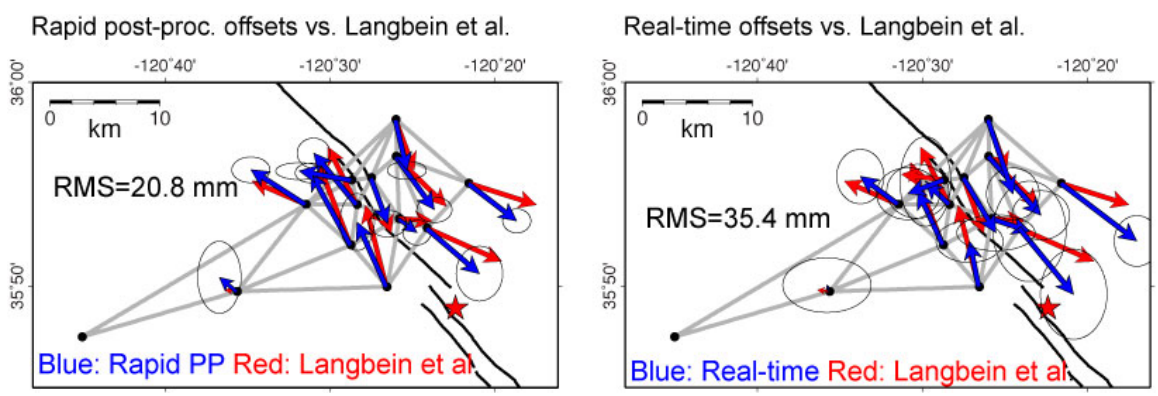

Figure 3: Comparison of offsets from simulated real-time processing (right) and rapid post-processing (left) to results from Langbein et al. [2006]. While both capture the overall characteristic of the deformation field, the RPP results have a better RMS misfit to the post-event analysis.

For all processing, we adopt a triangulated network strategy (e.g. grey lines in upper frame of Figure 2), where each baseline pair is individually processed using Track to determine the relative offset between two stations. This strategy makes the processing highly parallel, such that there is a minimal increase in time associated with individual pair processing. It also makes our network resilient against a data outage at any individual station and against the failure of any single processing instance. We have also tailored our fault parameter search to use these relative offsets directly, without performing a network adjustment that would cast each station's offset as relative to a single reference. Altering the model set-up to accept multiple relative offsets is fairly simply accomplished for a linear inverse problem. The major change is to cast the problem $\mathbf{Gm}=\mathbf{d}$ as $(\mathbf{G_1}-\mathbf{G_2})\mathbf{m}=(\mathbf{d_1}-\mathbf{d_2})$.

The static offsets measured from the RPP results for the Parkfield earthquake compare well with a post-event analysis by Langbein et al. [2006] (Figure 3). The simulated real-time results still capture the overall sense of motion and size of the Parkfield earthquake, but they do not compare as favorably to the Langbein et al. analysis. While the real-time offsets are likely to provide results that are good within uncertainties that are allowable for earthquake early warning, for response products that have the option to wait several minutes, RPP will provide better constrained fault parameters.

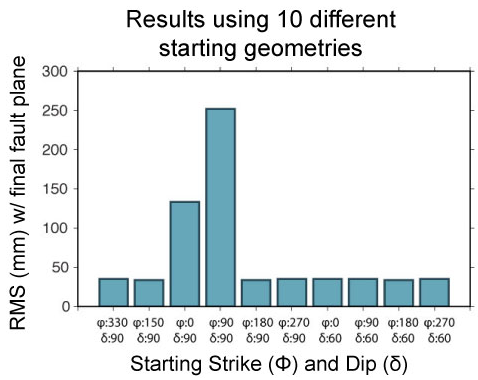

Figure 4: Histogram of results from 10 searches for best-fitting fault plane using 10 starting geometries for the Parkfield earthquake. 8 out of 10 find planes very similar to that shown in Figure 5.

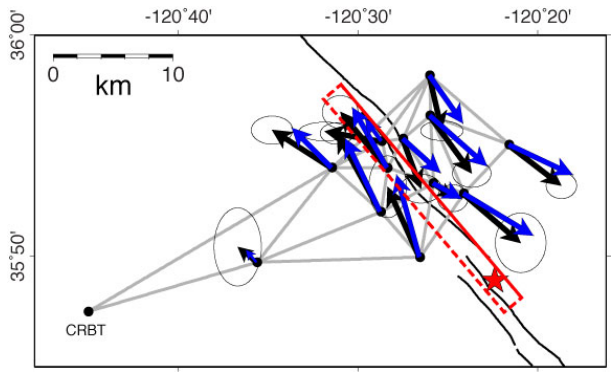

Figure 5: Best-fitting fault plane (red rectangle) with input data (blue vectors) and modeled results (black vectors) from RPP results for the 2004 Parkfield earthquake.

Estimating Fault Parameters

To find the finite fault parameters, we set up a nonlinear search including location, length, width, strike, dip and depth of the rupture plane, using no *a priori* information. That is, we attempt to simulate a situation where the type and location of faulting for the Parkfield earthquake is unknown. The current search method, using functions in Matlab, is sensitive to starting geometry and so we employ parallel processing of ten different starting geometries to investigate each's effect (Figure 4). The ten geometries include four different strike directions, two different dips and geometries parallel to the San Andreas fault system. Each starting geometry is centered on the earthquake epicenter and the starting width and length are based on relations from Wells and Coppersmith [1994]. We further constrain the inversion to require that the rupture plane be co-planar with the earthquake hypocenter.

Eight out of 10 starting geometries result in searches that find a rupture plane for the Parkfield earthquake that matches the orientation, dimensions, and location found by many investigators (Figure 5). The remaining two searches found local minima with final RMS values 10 times greater than the eight successful searches, allowing these to be easily excluded. Figure 6 shows how including the fault plane affects the ShakeMap calculations; including the RPP determined plane produces a ShakeMap that matches the final CISN ShakeMap well. However, while the finite plane used for the official ShakeMap matches the GPS determined plane, it was determined manually based on the aftershock distribution. As such is was several hours before this

information was incorporated into the ShakeMap. By contrast the same information can be obtained from GPS within 15 minutes.

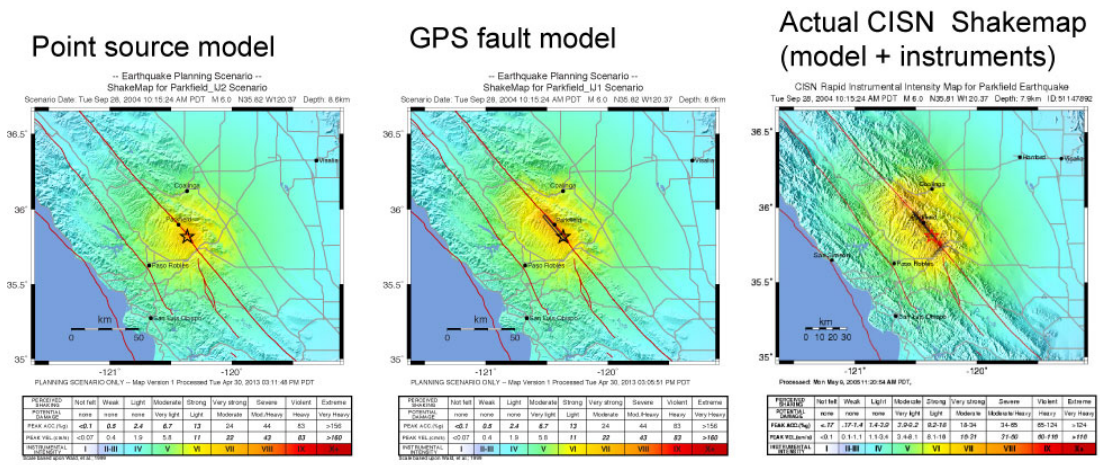

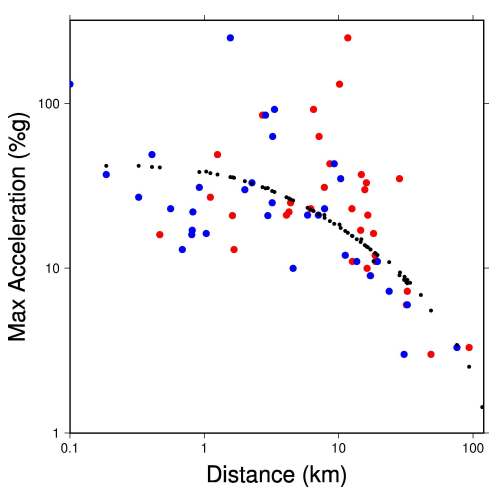

Figure 6 (Above): Three ShakeMaps for the 2004 Parkfield earthquake. The left and middle ShakeMaps are scenarios that contain only information from a distance/attenuation model. The right-most figure is the official CISN ShakeMap using both a model and instrumental data. Distance in the left-most figure is calculated to the earthquake epicenter only. In the middle plot, it is the closest distance to the fault plane.

Figure 7 (At left): Distance vs. maximum acceleration for stations given the point source (red points) and the finite fault (blue points). The black points show the modeled relationship. The difference between the red and blue points is in how the distance from the station to the earthquake is calculated.

Implementation in Northern California

While we hope that the method we have developed will be portable to GPS networks anywhere, we have first applied it to stations with real-time data access in Northern California. Real-time GPS data is available from over 60 stations in San Francisco Bay Area operated by several groups: The BSL's BARD network, the USGS, Menlo Park, and PBO. The Bay Area Regional Deformation (BARD) network of 32 permanent, continuously operating Global Positioning System receivers has been monitoring crustal deformation in the Bay Area and northern California since 1992 [*Murray et al.*, 1998; *Houlié and Romanowicz*, 2011]. All BARD stations are continuously telemetered to the BSL at 1 Hz sampling rate, and are streamed in real time over a Ntrip-caster, where they are available to the public (http://seismo.berkeley.edu/bard/realtime). We also share data with the USGS, Menlo Park, such

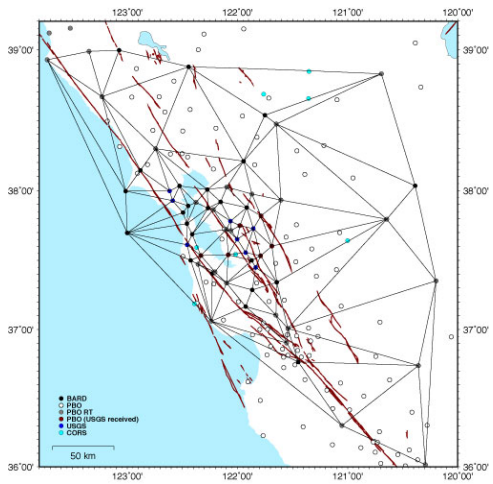

Figure 8: Current real-time processing and RPP network. Each line represents an individual station pair to be processed independently.

that each agency has immediate access to each other's data. Even though the data are post-processed, our method still relies on real-time data access. It is not feasible to retrieve data from remote GPS stations in the "rapid" time frame, so the RPP processing network effectively mirrors the real-time processing network (Figure 8).

References

Cohee, B. P., and G. C. Beroza (1994), Earth-prints: A comparison of two methods for earthquake source inversion using strong motion seismograms, *Annals of Geophysics*, *37*(6), 1515–1538.

Dreger, D. S., L. Gee, P. Lombard, M. H. Murray, and B. Romanowicz (2005), Rapid Finite-source Analysis and Near-fault Strong Ground Motions: Application to the 2003 Mw 6.5 San Simeon and 2004 Mw 6.0 Parkfield Earthquakes, *Seismol. Res. Lett.*, *76*(1), 40–48, doi:10.1785/gssrl.76.1.40.

Houlié, N., and B. Romanowicz (2011), Asymmetric deformation across the San Francisco Bay Area faults from GPS observations in Northern California, *Physics of the Earth and Planetary Interiors*, *184*, 143–153.

Johanson, I. A., and R. Bürgmann (2010), Coseismic and postseismic slip from the 2003 San Simeon earthquake and their effects on backthrust slip and the 2004 Parkfield earthquake, *J. Geophys. Res.*, *115*(B7), doi:10.1029/2009JB006599.

Kim, A., and D. S. Dreger (2008), Rupture process of the 2004 Parkfield earthquake from near-fault seismic waveform and geodetic records, *J. Geophys. Res.*, *113*(B7), doi:10.1029/2007JB005115.

Langbein, J., J. R. Murray, and H. A. Snyder (2006), Coseismic and Initial Postseismic Deformation from the 2004 Parkfield, California, Earthquake, Observed by Global Positioning System, Electronic Distance Meter, Creepmeters, and Borehole Strainmeters, *Bull. Seismol. Soc. Am.*, *96*(4B), S304–S320, doi:10.1785/0120050823.

Larson, K., P. Bodin, and J. Gomberg (2003), Using 1-Hz GPS data to measure deformations caused by the Denali fault earthquake, *Science*, *300*(5624), 1421–1424.

Murray, M., R. Bürgmann, W. Prescott, B. Romanowicz, S. Schwartz, P. Segall, and E. Silver (1998), The Bay Area Regional Deformation (BARD) permanent GPS network in northern

California, *Eos Trans AGU*, *79*(45).
Murray-Moraleda, J. R., and R. W. Simpson (2009), Geodetically Inferred Coseismic and Post-seismic Slip due to the M 5.4 31 October 2007 Alum Rock Earthquake, *Bull. Seismol. Soc. Am.*, *99*(5), 2784–2800, doi:10.1785/0120090017.
Rolandone, F., D. Dreger, M. Murray, and R. Bürgmann (2006), Coseismic slip distribution of the 2003 Mw6.6 San Simeon earthquake, California, determined from GPS measurements and seismic waveform data, *Geophys. Res. Lett.*, *33*(16), L16315, doi:10.1029/2006GL027079.
Wald, D. J., V. Quitoriano, T. H. Heaton, H. Kanamori, C. W. Scrivner, and C. B. Worden (1999), TriNet "ShakeMaps": Rapid generation of peak ground motion and intensity maps for earthquakes in southern California, *Earthquake Spectra*, *15*(3), 537–555.
Wald, D., K.-W. Lin, K. Porter, and L. Turner (2008), ShakeCast: Automating and Improving the Use of ShakeMap for Post-Earthquake Decision-Making and Response, *Earthquake Spectra*, *24*(2), 533–553, doi:10.1193/1.2923924.
Wells, D. L., and K. J. Coppersmith (1994), New empirical relationships among magnitude, rupture length, rupture width, rupture area, and surface displacement, *Bull. Seismol. Soc. Am.*, *84*(4), 974–1002.

Publications from this work

Johanson, I. A., Grapenthin, R. (in preparation), Rapid finite-fault information from real-time GPS data for ShakeMap